

THE DYNAMICAL TRANSITION IN PROTEINS: THE ROLE OF HYDROGEN BONDS

Wolfgang DOSTER and Marcus SETTLES*

*Technische Universität München, Physikdepartment E13, D-85748 Garching,
Institut für Röntgendiagnostik, Klinikum rechts der Isar, D-81675 München

Abstract. The onset of anharmonic molecular motions in proteins is shown to depend on fluctuations of intramolecular- and protein-water hydrogen bonds. Energy-resolved neutron scattering and Mößbauer spectroscopy reveal two anharmonic dynamical components: fast side-chain librations and a less localized reorganisation of the hydrogen bond network. The former involve two levels in the hierarchy of conformational substates: A glassy state, where the side-chains are locked by rigid hydrogen bonds and a liquid state where the bonds fluctuate on a picosecond time scale. The change in the population of the two states ($\Delta H \approx 10$ kJ/mol) causes a transition in the dynamic properties.

1. Background

A complete description of proteins and their complexes in aqueous solution involves three separate aspects: structure, energetics and dynamics. These areas are studied by very different methods and have progressed to a large extent independently of each other. The first attempts at their synthesis are being carried out by means of lengthy and up to now tentative computer simulations. Below we outline a complementary experimental approach by means of energy-resolved scattering techniques combined with studies covering a wide range of temperatures.

What discriminates proteins from other non-biological polymers is the ability to assume a soluble, compact state in water. The rigidity required to maintain a well defined structure is achieved by excluding water at a concentration of 55 M from a protein's interior. Most proteins contain a central core formed by one or several clusters of close-packed nonpolar side chains. The stability of the core depends critically on van der Waals interactions which are of short range. Thus fluctuations away from the compact state are dangerous and have to be small in size. Volume fluctuations in dense systems are generally controlled by repulsive forces. For proteins such motions are best pictured as a self-avoiding jostling of side-chains. The corresponding relaxation of local volume fluctuations resembles the adjustments carried out by a dense crowd in a tramway when a new passenger moves in.

As an example consider the binding of a small molecule like dioxygen to myoglobin. What makes the problem interesting is that the examination of the high resolution x-ray structure of myoglobin does not reveal any path by which the ligand can reach the heme

binding site from the solvent [1]. Since this holds true for both the deligated and the liganded protein, structural fluctuations must be involved in the entrance and exit of dioxygen. Empirical energy function calculations have shown that the rigid protein would oppose ligand displacements by barriers on the order of 100 kcal/mol [2]. In a rigid world, oxygen binding would take an infinitely long time on a biological scale. In real life, at least the one which can be simulated on the computer, barriers can relax by structural adjustments. The calculated relaxed barrier heights for particular ligand trajectories turned out to be on the order of 10 kcal/mol, similar in size than those found in flash photolysis experiments with oxy-myoglobin [3]. This example illustrates why the popular view of protein conformational dynamics, the conformational migration across a complex, but fixed energy landscape [4], should be applied with care to local processes. Displacements of molecular groups on a local scale are affected by fluctuating barriers. This situation is closely related to motions of particles in a liquid: The average structure of a liquid appears to be close-packed and does not reveal the essence of the liquid state, the ease of molecular diffusion. Moreover, the average structure of a liquid is not significantly different from the one of the corresponding glass, the difference in the mechanical properties is however dramatic [5].

Diffusion on a molecular scale is a complex process which, as in the case of the crowded tramway, requires the collective rearrangement of the cage formed by the nearest neighbours of each 'particle'. When a critical density is approached from below, the cage turns into a trap. The particle cannot move because the neighbours cannot move, the neighbours cannot move because their neighbours cannot move etc. As a result structural fluctuations become arrested up to macroscopic scales. The success of mode coupling theory in establishing a self-consistent description of the cage effect, supported now by numerous experimental results, lead to a new microscopic understanding of the liquid to glass transition [6,7]. The theory has implications on all dense systems where the cage effect plays a dominant role. It predicts in particular a nonlinear increase in the mean square displacements on approaching a critical temperature from below. The transition is truly dynamical in nature, a continuous change in the structural properties leads to a discontinuous behaviour in the long time dynamics. The density fluctuations which are arrested at low temperatures, can decay above the critical temperature.

The relevance of this approach to proteins has been demonstrated by neutron scattering experiments, the spectra of fast protein motions strongly resemble those observed with supercooled liquids [8,9]. The density correlation function was shown to decay in two steps, a fast motion of side chains ratteling in their local cage and slower displacements of longer range associated with the transition to a new position. These processes are closely related to the fast β - and α -relaxation of liquids. The most interesting result with proteins was the observation of a transition in the dynamical properties analogous to the liquid to glass transition [10,11,12]. The differences and common features have been discussed by Sartor et al. and Green et al. [13,14]. The common phenomenology may reflect the dense packing and thus the dominant influence of short range repulsive forces on protein motions. This kind of strictly intramolecular transition may apply to dehydrated proteins or in vacuo MD-simulation of myoglobin [11,15,16] and bacteriorhodopsin [17,18].

In addition to van der Waals forces we have to consider electrostatic interactions which are of long range. Most important are hydrogen bonds which can stabilize the protein against large scale excursions from the average structure. The people in the tramway want to be surrounded by their friends. If a major disturbance occurs, they will try to restore their equilibrium configuration by long range interactions. It is not too surprizing that large amplitude displacements in proteins are mediated by hydrogen bonds.

Such motions then appear as the dominant contribution in inelastic scattering spectra. Another important property of hydrogen mediated electrostatic interactions is their directionality and the fact that they can be saturated. Taken together these properties allow us to operate with notions like open or broken and closed hydrogen bonds, although there is no well defined cut-off distance [19]. In order to move, bonds have to be broken. The network of bonds establishes another cage mechanism which resists motion. Lowering the temperature leads to thermal contraction, the bonds length decreases.

As a result the bonds become stronger, in addition, the thermal energy available to brake the bond also decreases [20]. We may thus expect a second kind of dynamical transition associated with hydrogen bonds and in particular protein-water H-bonds.

Nearly all polar groups in proteins form hydrogen bonds either with each other or with water. In myoglobin, about 180 hydrogen bonds between side chains and water were identified by X-ray and neutron crystallography [21,22]. A comparable number, 193 of such bonds were detected between main chain amide groups and water. Taken together the protein-water bonds outnumber the 256 intramolecular H-bonds between the main chain amides in myoglobin. Moreover the intermolecular bonds are easily broken due to interactions with bulk water molecules.

Myoglobin is composed of a single domain, which contains a cluster of 8 α -helices. This protein proved to be an excellent model system, to study dynamics. Its functional properties, the kinetics of ligand binding, can be probed by flash photolysis within a wide range of temperatures and solvent conditions [23]. Most important, the dynamics of the active site, the heme group, can be monitored by Mößbauer spectroscopy [12]. Overexpression of the myoglobin gene in E.Coli made mutant studies possible [38]. Most proteins are composed however of several structural domains or subunits. In many cases it is the binding of a bulky ligand which triggers the transition from a closed structure to a less compact state. The open-closed transition, however rarely involves the deformation of van der Waals clusters. Instead, more often than not, two non-polar protein domains, dressed by polar side chains, move relative to each other [24]. This process involves a specific reorganization of the H-bond network. We thus have to understand the contribution of H-bonds to protein plasticity on a very basic level.

2. Mean Square Displacements derived from elastic scattering experiments

In energy resolved scattering experiments with proteins one measures spectra composed of an elastic fraction related to events without energy exchange and inelastic components which reflect the dynamics of the particles. The elastic intensity $I_{el}(Q)$, is proportional to the value of the scattering function $S(Q,\omega)$ at frequency $\omega = 0$. $I_{el}(Q)$ is frequently used to get an estimate of the molecular displacement amplitudes. Q denotes the length of the scattering vector. $I_{el}(Q)$ can be considered as a measure of the probability that a particle does not move across a length scale $1/Q$ within a time interval given by the energy resolution of the instrument. If the displacements are isotropic and Gaussian distributed one may write [24]:

$$I_{el}(T,Q)/I_{el}(T_0,Q) \approx \exp(-Q^2\langle\Delta x^2\rangle_{eff}) \quad (1)$$

In coherent scattering experiments, for instance with x-rays, the $\langle\Delta x^2\rangle_{eff}$ contain a static component due to disorder, while the displacements are entirely dynamic in nature for incoherent events. The latter applies to neutrons scattering by hydrogens and the Mößbauer resonance absorption of γ -quanta. The experimental data are usually normalized to an elastic intensity obtained at a low temperature T_0 . One has to keep in mind that this procedure removes the zero point vibrations. For vibrational motions equ.(1) is called the

Debye-Waller factor. The elastic intensity provides a reasonable measure of the elastic fraction for well resolved processes only. The elastic intensity in general depends on the instrumental resolution function, $R(\omega, \Delta\omega)$:

$$S(Q, \Delta\omega, \omega = 0) = \exp(-Q^2 \langle \Delta x^2 \rangle_{\text{vib}}) \int d\omega' S_{\text{quell}}(Q, \omega') R(\omega', \Delta\omega) \quad (2)$$

$\hbar\Delta\omega$ is the full width at half maximum of $R(\omega, \Delta\omega)$. $S_{\text{quell}}(Q, \omega)$ denotes the dynamical structure factor of slow, non-vibrational motions. The effective displacements $\langle \Delta x^2 \rangle_{\text{eff}}$ in equ.1 thus carry the time tag of the instrumental resolution, $\tau_{\text{res}} \approx 2/\Delta\omega$ and are called elastic. Fig.1 shows the elastic scans of the peptide alanine, which has a methyl group as the side-chain, alanine dipeptide, which has in addition two terminal methyl groups, and of hydrated lysozyme: The methyl group in the alanine crystal is blocked and can only

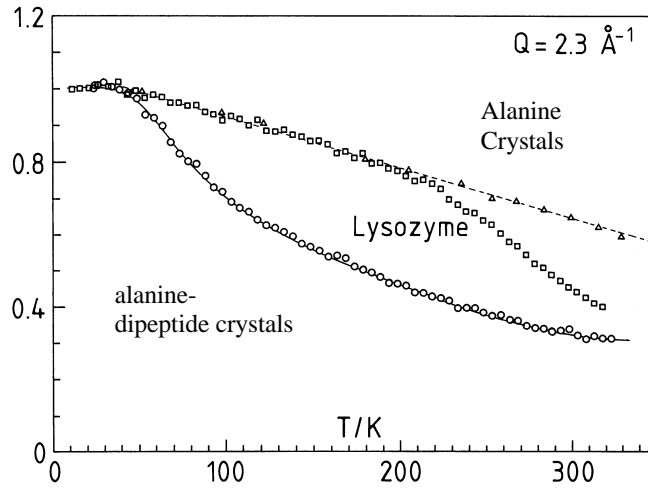


Figure 1: Elastic intensity normalized at 4 K, $I_{\text{el}}(T, Q)/I_{\text{el}}(4 \text{ K}, Q)$, of alanine crystals, D_2O -hydrated lysozyme and alanine-dipeptide at a fixed time window of $\tau \approx 80 \text{ ps}$ (IN13, ILL). The dashed line corresponds to harmonic behaviour. the full line represents a fit to the elastic scattering function of the dipeptide assuming rotational jumps of the three methyl groups. The activation energies ΔH are 2.5 kJ/mol and 3.0 kJ/mol for the N- and C- terminal methyls and 11 kJ/mol for the side chain methyl group, prefactors are $2 \cdot 10^{13} \text{ s}^{-1}$

vibrate around the minimum of the rotational potential consistent with the harmonic temperature dependence of $I_{\text{el}}(T, Q)$: $I_{\text{el}}(T, Q) \approx 1 - Q^2 \langle \Delta x^2 \rangle_{\text{eff}}$ with $\langle \Delta x^2 \rangle_{\text{eff}} = \langle \Delta x^2 \rangle_{\text{vib}} \propto T$.

The C- and N-terminal methyl groups of the dipeptide exhibit much lower potential barriers than the side-chain [29]. They perform rotational jumps on a 100 ps time scale above 40 K which is resolved by the instrument. The resulting inelastic scattering leads to a decrease in the elastic intensity above 40 K. The fits to the elastic scans of the dipeptide data were performed using equ.(2), with the structure factor of the methyl rotation [25] and the instrumental resolution function as input. All three methyl groups contribute to the loss in elastic intensity with onset-temperatures depending on the rotational potential and the instrumental resolution. In contrast, the onset of the intensity decrease at 180 K in the case of hydrated lysozyme does not depend on the instrumental resolution. This time scale independence together with the absence of an associated structural change are characteristic features of a dynamical transition. Fig.2 shows the resulting effective mean square displacements of hydrated lysozyme at 12 ps (IN6) and 80 ps (IN13). The onset temperatures of anharmonic motions, 180 K, are identical. But the displacements diverge above 220 K reflecting larger excursions depending on the time of observation.

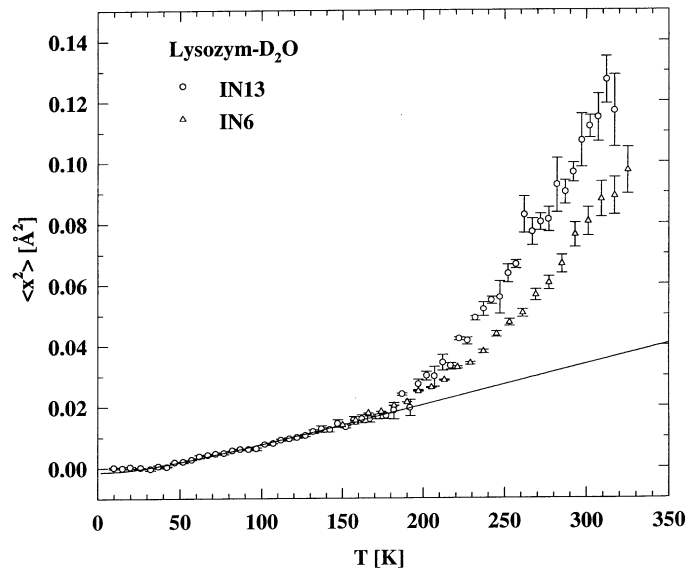


Figure 2: Elastic mean square displacements of D₂O-hydrated lysozyme (0.35 g/g) obtained at two elast resolutions $\tau_{\text{res}} \approx 80$ ps (IN 13) and 12 ps (IN 6). The full line represents the vibrational displacements determined from the measured vibrational density of states. No adjustments except for the removal of the zero point vibrations were made.

Fig.3 shows the mean square displacements of D₂O-hydrated myoglobin using different instrumental resolutions: Neutron scattering probes the nonpolar hydrogens, essentially the side-chains, with $\tau_{\text{res}} \approx 10$ ps and 80 ps. The γ -resonance absorption experiment probes the displacements of the heme iron up to 140 ns. The onset temperatures, about 180 K are identical in spite of several orders in magnitude difference in τ_{res} . Note however that above

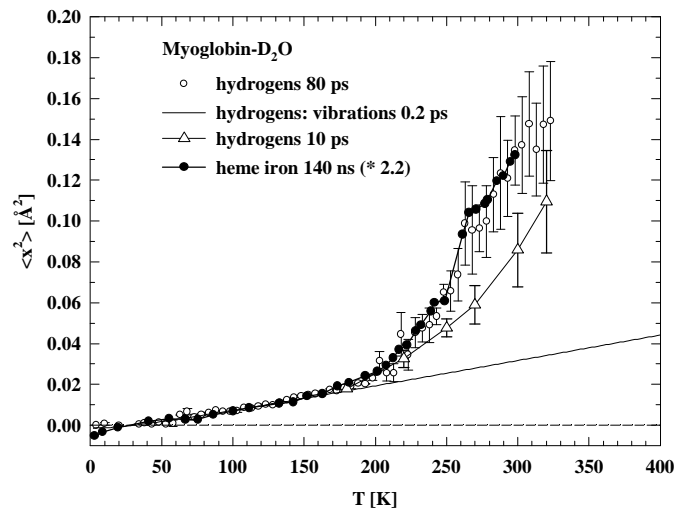


Figure 3: Mean square displacements of hydrated myoglobin (neutron scattering), reflecting the nonpolar hydrogen on the indicated time scales (instruments IN13 and IN6) [10,31] and Mössbauer spectroscopy of the heme iron [29]. The iron displacements were upscaled by a factor 2.2 to superimpose with the neutron data in the low temperature range.

220 K, longer observation times also lead to larger apparent displacements as expected. Neutron scattering allows a well defined determination of the displacements from the initial slope of $I_{el}(Q)$. In general this requires multiple scattering corrections [31]. The technique however cannot discriminate the extra motions of the hydrogens from those of the heavy atoms to which they are attached. The γ -resonance absorption experiment refers to a single Q value of 7.2 \AA^{-1} , which is larger than those achieved with thermal neutron scattering. The Mössbauer effect is very sensitive to motions on a small scale. In order to derive $\langle \Delta x^2 \rangle_{eff}$ from the elastic intensity, one has to assume isotropic, Gaussian dynamics, $\langle \Delta x^2 \rangle_{eff} = - (\ln I_{el} / 7.2^2) \text{ \AA}^2$. Anisotropic motions and structural heterogeneity will be underestimated with this procedure. The resulting values of $\langle \Delta x^2 \rangle_{eff}$ should thus be considered as lower limits.

3. The Effect of Water on Protein Structural Displacements

In the following we focus on the analysis of incoherent neutron scattering data obtained with hydrated myoglobin. The scattering by water can be emphasized or suppressed since D_2O has a much lower neutron cross section than H_2O . To elucidate the coupling of water to protein motions we investigate samples at different degrees of hydration. Fig.4 shows the resulting displacements obtained with myoglobin at low and intermediate hydration. In previous work we have shown that the asymmetric two-state model (fig.4, insert) fits the $I_{el}(Q,T)$ data remarkably well and provides a first approximation to characterize the geometry and energetics of the nonharmonic displacements [10,14].

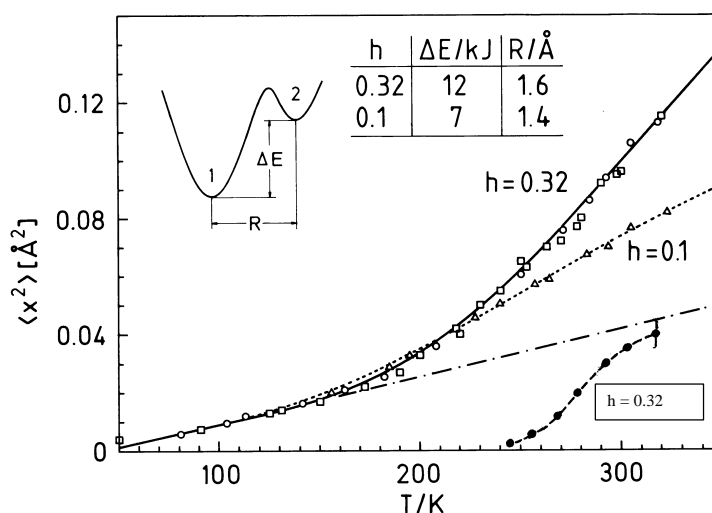


Figure 4: Elastic displacements of myoglobin at 0.32 and 0.1 g/g D_2O /protein, evaluated using the two state model (insert and equ.3) [11,15]. Open squares and circles correspond to two data sets, the closed circles reflect the extra displacements observed for $h = 0.32$ only, at high Q . The full and dotted lines are fits to the model, the energy difference $\Delta E = \Delta H$ and the jump length $d = R$ are given in the insert.

Instruments: ILL, IN13, $\tau_{res} \approx 80$ ps.

Both, the hydrated and the dehydrated protein exhibit a dynamical transition. Moreover, the corresponding transition temperatures, ≈ 180 K, are nearly identical. This suggests that the transition reflects the onset of solvent-decoupled intramolecular displacements.

The motional amplitudes of dry and hydrated myoglobin coincide up to 240 K. Above this temperature they diverge, indicating that the hydration of the polar surface induces extra displacements which are not present in the dry case. Moreover, the extra motions above 240 K correlate with the onset of a new process (full circles, fig.4) which is also not seen in the dry system. [11,15]. Surprisingly similar results were found for the heme iron of hydrated and dehydrated myoglobin with Mössbauer spectroscopy [33,30].

What is the molecular nature of these motions? The protein displacements depend on the number of water molecules which points to fluctuations of the hydrogen bond network as the basic dynamic mechanism [10,20]. As a simple model of this process we first assume just two states for each hydrogen bond, open and closed. To brake the bond requires an energy ΔH . The open/closed state population is then controlled by the Boltzmann factor, $\rho = \exp(-\Delta G/RT)$, $\Delta G = \Delta H - T\Delta S$. We associate with this process a displacement, d , of nonpolar hydrogen atoms in the side-chains. We further assume that bond-formation is fast (ps) and nearly activationless. This model predicts an exponential increase in the motional amplitudes with the temperature $\langle \Delta x^2 \rangle \propto \rho(T)$, while the relaxation rate, which is dominated by the fast bond formation, remains fixed. The dynamical transition in this view reflects the increasing amplitude of fast bond fluctuations which become comparable in size to the vibrational displacements. This explains why the transition occurs at a fixed temperature provided that τ_{res} , the observation time is longer than a few picoseconds. The resulting energy asymmetry of about 10 kJ/mol (fig.4, insert), is a typical value for hydrogen bonds of intermediate strength. The assumption of exactly two states should be considered with a grain of salt. It accounts for the data taken at low hydration. For the hydrated system a small entropic term of $\Delta S/R = 3$ was required to fit the data.

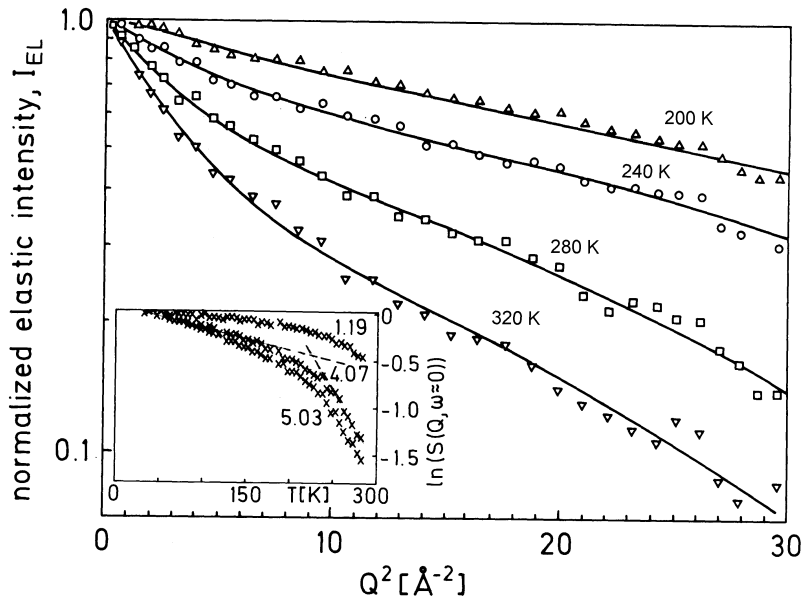


Figure 5: Elastic intensities $I_{el}(Q,T)$ of D_2O -hydrated myoglobin, the lines represent fits to equ.(3), the parameters are given in fig.4. The insert shows the elastic scans versus temperature at several Q -values. The dashed lines denote the limiting slopes related to Gaussian displacement amplitudes. Note the twofold change in the slope at high Q .

The two-state model leads to following the powder averaged scattering function [11]:

$$I_{el}(Q, T) \approx \exp(-Q^2 \langle \Delta x^2 \rangle_{vib}) \frac{1}{(1+\rho)^2} (1+\rho^2 + 2\rho j_0(Qd)) \quad (3)$$

$j_0(x)$ denotes the zero order Bessel function $\sin(x)/x$. Fig. 5 shows fits of $\ln(I_{el})$ versus Q^2 which deviates from a straight line above 200 K. Equ.(3) allows to reproduce the non-Gaussian shape of $I_{el}(Q, T)$ which emerges above 200 K rather well. The resulting hydrogen jump length of $d = 1.6 \text{ \AA}$ (fig. 4) is comparable to those observed for the hydrogen atoms in flip-flop motions of water molecules near polar surfaces [34]. The smaller displacements observed at low hydration are interpreted in this model as the combined action of a lower hydrogen bond strength and a shorter jump length of the side-chain hydrogens. This result seems self-contradictory because reducing the constraints should enhance the motional amplitudes. Although the model catches several important aspects of the system, it does not account for the heterogeneity of local interactions in the protein structure: All hydrogens are assumed to be dynamically equivalent. The protein surface however, will respond differently to changes in hydration than the side chains buried in the protein interior. This suggests another interpretation of the scattering function (equ.3) in terms of two dynamical components: A mobile fraction, $f_\beta(T) = 2\rho/(1+\rho)^2$, and an rigid component, $1-f_\beta = (1+\rho^2)/(1+\rho)^2$ which performs only vibrational motion. We further approximate the elastic intensity in fig.(5), the two slopes, by a sum of two Gaussian components:

$$I_{el}(Q, T) = f_\beta(T) \exp(-Q^2 \langle \Delta x^2_\beta \rangle) + (1 - f_\beta) \exp(-Q^2 \langle \Delta x^2_{vib} \rangle) \quad (4)$$

The open state of the above asymmetric two-state model is now interpreted as the fraction of mobile side chains which are surrounded by fluctuating hydrogen bonds. The closed state refers to the fraction of side chains which are constrained by rigid H- bonds. The population of the mobile fraction depends on the Boltzmann factor, $\rho(T)$:

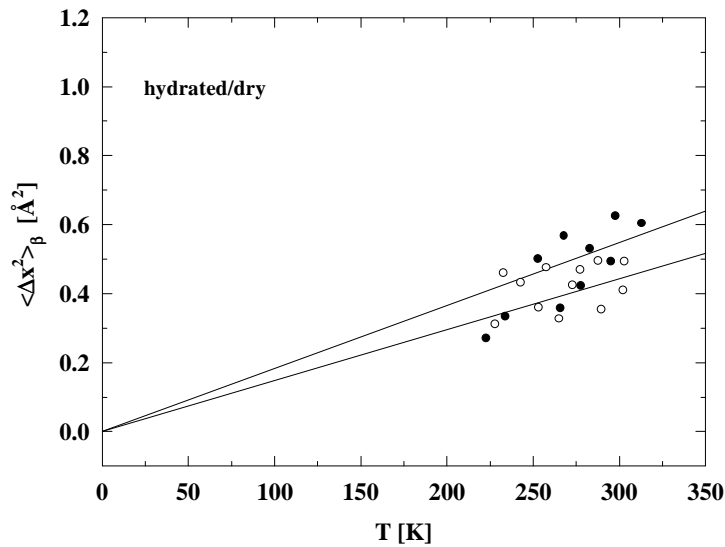


Figure 6a: The mean square displacements of the β -process evaluated in the two component model of equ. (4). full circles: hydrated myoglobin $h=0.35$, open circles: $h=0.1\text{g/g}$. The full lines imply harmonic displacements ($\propto T$) on a softer potential surface.

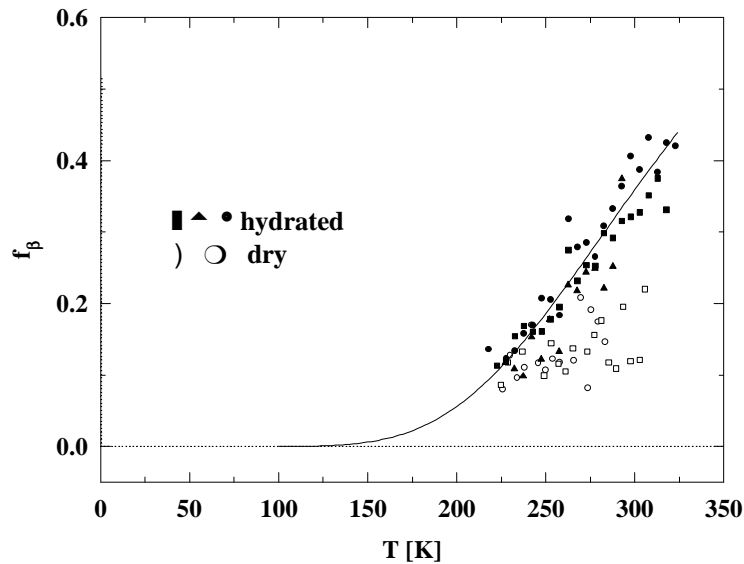
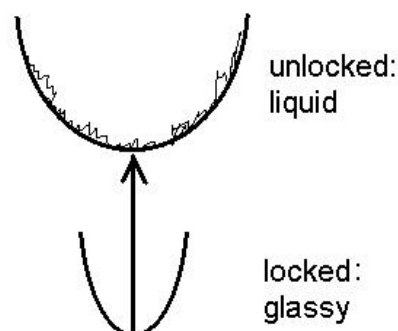


Figure 6b: The fraction of mobile hydrogens due to the β -process $f_{\beta}(T)$ of dry and D_2O -hydrated myoglobin and lysozyme, evaluated according to equ. 4. The full line is at fit to $\rho(T)$ yielding $\Delta H = 10$ kJ/mol and $\Delta S/R = 4$.

Complementary models were proposed for hydration water and heme dynamics [43,44]. The ‘ β ’ implies that we consider the anharmonic side-chain librations in the context of a glass transition scenario as a fast β -process. The result of the new analysis of the scattering function (equ.4) is shown in fig.(6a): The amplitude of the side-chain librational displacements are now independent of the degree of hydration in contrast to the homogenous model.

The full lines imply a linear temperature dependence and thus harmonic behaviour related to a softer potential surface. The nonharmonic temperature dependence is now attributed to a change in the population of mobile side-chains. The following picture emerges: A protein side-chain can assume two dynamical states, glassy and liquid-like, depending on whether the local network is fluctuating on a picosecond time scale or not. Fits to the data in fig.(6b), assuming $f_{\beta} \propto \rho(T)$, yields in the hydrated case $\Delta H = 10$ kJ/mol which is a typical energy required to brake one hydrogen bond. The side-chains are constrained at



low temperatures by rigid bonds and perform underdamped high frequency oscillation. With increasing temperature the force constants soften, the bonds start fluctuating. This creates a new effective potential surface, characterized by a lower vibrational frequency in a range where fast dissipative processes can interfere.

The β -process, which triggers the onset of anharmonicity, has still very much in common with vibrational motions. Vibrations give rise to a quantum analogon of the dynamical transition: The elastic intensity in fig.(1) starts to decrease above 30 K, when the displacements due to thermally populated vibrational states become comparable to the zero point vibrations. Furthermore, the population changes with the temperature according the Bose occupation factor, while the characteristic frequencies remain constant: $f_{\text{vib}}(T) = 1/[\exp(\hbar\omega/K_B T) - 1]$.

Increase in hydration enhances the fraction of mobile side-chains at a given temperature (Abb. 6b). Hydrogen-bonds can flip only in the presence of alternative acceptors. Adding water molecules introduces new sites. This suggests that the observed extra mobility (fig. 4) reflects the lubricated polar side chains at the protein-water interface.

The extra mobility of the hydrated system displayed above 240 K coincides with the emergence of a new process as shown in fig. 4 (filled circles). This feature reveals itself in fig. 5 as a further decrease in the elastic intensity (insert) and in the larger slope of $I_{\text{el}}(Q,T)$ at high Q in excess of $\langle \Delta x^2 \rangle_{\text{vib}}$ (equ.4). To connect to similar phenomena in undercooled liquids, we call this new process, which is not observed at low hydration, the structural or α -relaxation of the protein-water system. The α -process, to a larger extent than the β -process, involves fluctuating barriers due to the collective rearrangement of many particles. Both processes are however intimately related: The fast bond fluctuations provide the local mobility required for rearrangements on a larger spatial and temporal scale. Elastic intensities allow to derive displacements with a fixed time tag only. Inelastic spectra allow to determine time-resolved displacements as discussed in [41].

4. Inelastic neutron scattering spectra of side-chain fluctuations

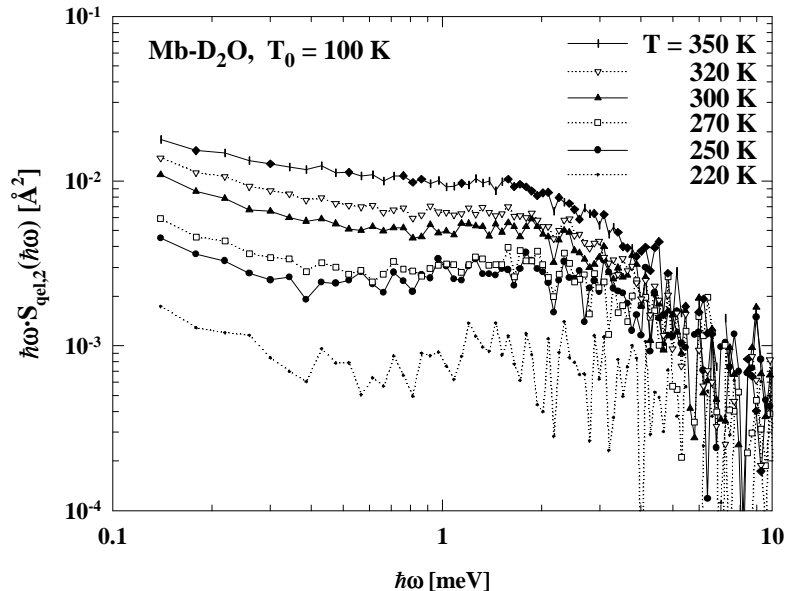


Figure 7a) The susceptibility spectrum of hydrated myoglobin derived from the $Q \rightarrow 0$ extrapolated the density of states. A harmonic vibrational background has been subtracted (100 K). The broad peak at about 2 meV reflects the β -process. Instrument: ILL, IN6, $\lambda = 5.2 \text{ \AA}$ [9,32].

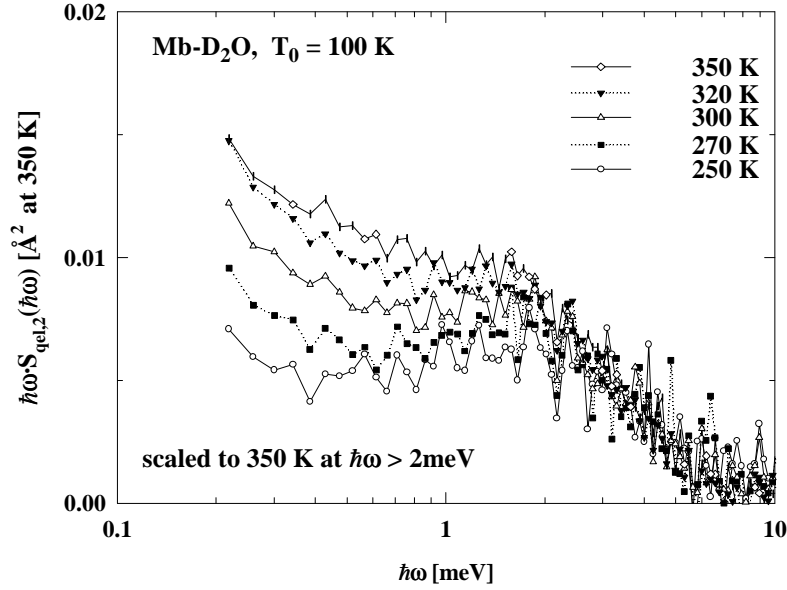


Figure 7b) Quasielastic susceptibilities in the β -process region derived from the $Q \rightarrow 0$ extrapolated density of states of D_2O -hydrated myoglobin as in fig.7a.

The spectra were rescaled to the high frequency wing of the data at 350 K.

From the analysis of the elastic intensity above, we deduce the existence of a fast β -process with the following properties: The β -amplitude increases exponentially with the temperature, but the shape and position of the spectrum remain approximately constant. Fig.(7a) shows a susceptibility spectrum of the β -process which exhibits a broad maximum at 2 meV (≈ 0.5 ps) [9,32]: The minimum and the intensity increase at lower energy reflect the high frequency wing of the α -relaxation. The β -spectrum shows the expected features. To remove the effect of bond fluctuations we rescale the spectra by a temperature dependent factor $\propto f_\beta(T)$. The resulting spectra, shown in fig.(7b), exhibit a residual temperature dependence due to the α -process. From $f_\beta(T) \propto \rho(T)$, we derive an energy difference between the locked and the unlocked state, of $\Delta H \approx 10.5$ kJ/mol which is in agreement with the analysis of the elastic intensity.

To illustrate how the α -relaxation and the β -process are likely to be connected, we invoke a concept which explains most of the unusual properties of bulk water [35,36]: Water is considered to be a percolating network of transient bonds. Computer simulations suggest that water molecules can be classified according to the number of H-bonds that connects them to their nearest neighbours. Only those molecules without bonds can diffuse at a given time. The bulk diffusion coefficient is thus proportional to the fraction of molecules with zero bond. The mobile fraction was denoted by f_β . We write the α/β spectrum as a sum of two Lorentzians with amplitude $1 - f_\beta$ and f_β respectively. Most important: The α -relaxation rate, the elementary step of diffusion, is set to be proportional to f_β , the mobile fraction. Thus, $1/\tau_\alpha = C f_\beta$. The result is:

$$S(\omega, T) = (1 - f_\beta) \frac{C f_\beta}{\omega^2 + (C f_\beta)^2} + f_\beta \frac{1/\tau_\beta}{\omega^2 + (1/\tau_\beta)^2} \quad (5)$$

the Q -dependence and a factor $1/\pi$ are omitted. Since $\tau_\alpha \gg \tau_\beta$, the spectrum at high frequencies ($\omega \gg C f_\beta$) scales with $f_\beta(T)$ ($\ll 1$), while its shape remains constant:

$$S(\omega, T) \approx f_\beta(T, h) \left(\frac{C}{\omega^2} + \frac{1/\tau_\beta}{\omega^2 + (1/\tau_\beta)^2} \right) \quad (6)$$

Equ.(6) is in accord with the high frequency neutron scattering spectra of dry and hydrated myoglobin which differ only by a frequency independent factor, $f_{\beta}(h)$ [24]. The rescaled spectra in fig.(7b) are not constant however, suggesting a residual temperature dependence of $C = C(T)$ and thus a non-Arrhenius $\tau_{\alpha}(T)$.

5. Thermal expansion and strength of hydrogen bonds

We now look directly at the temperature evolution of the protein-water hydrogen bonds using infrared spectroscopy. The O-H stretching vibration of O-H...O depends sensitively on the inter-oxygen distance. Increasing the distance weakens the bond which in turn increases the O-H force constant and thus the stretching frequency ν_{OH} . Technically, to avoid the saturation of the detector, one uses partially deuterated water which yields the O-D stretch, ν_{OD} . Fig.8 shows the temperature evolution of the O-D stretching vibration of partially deuterated hydration water of myoglobin [10,20].

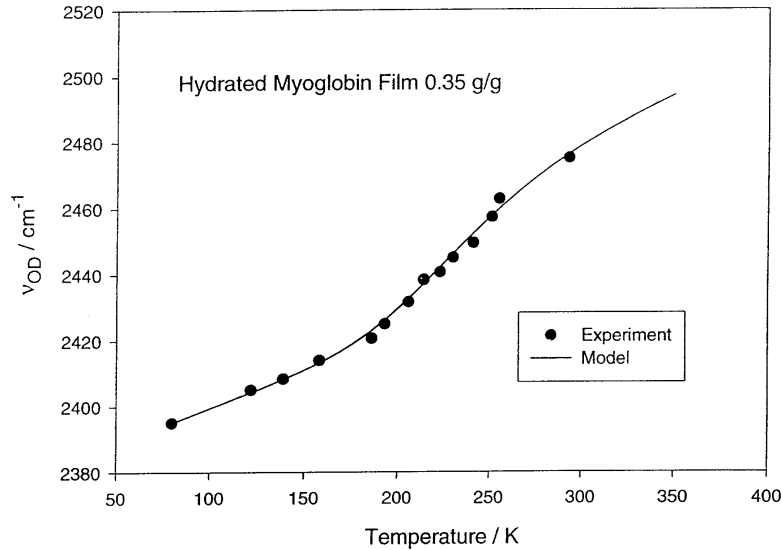


Figure 8: O-D stretching frequency, ν_{OD} , of partially deuterated hydration water of myoglobin. The full line represents a fit to a two state model:

$\nu_{OD} = f \nu_{OD}(\text{open}) + (1-f) \nu_{OD}(\text{closed})$. f denotes the fraction of fluctuating bonds. $\nu_{OD}(\text{closed}, T)$ was approximated by a linear temperature dependence, while the $\nu_{OD}(\text{open})$ was kept fixed at 2510 cm^{-1} , the value of bulk H-O-D.

The linear increase of ν_{OD} at low temperatures reflects the thermal expansion due to the anharmonicity of the closed H-bond. Above 180 K, we observe an extra expansion which is interpreted as the onset of bond fluctuations. This effect seems to be directly related to the dynamical transition observed in the mean square displacements of hydrated proteins at about the same temperature (figs.2,3). Assuming again a two-state equilibrium of fluctuating and rigid bonds we can fit the data with $\Delta H = 14 \text{ kJ/mol}$ and $\Delta S/R = 7$.

6. Dynamics of the heme iron and the kinetics of ligand binding to myoglobin

In the biological context it is of central importance to understand how side-chain fluctuations modulate the active site and functional properties such as the kinetics of ligand binding. It is also of interest whether these features appear only with hydrated proteins or whether proteins in other solvents exhibit a similar transition. To answer this question we studied the kinetics of ligand binding and the dynamics of the heme group of myoglobin in various solvents [23, 37]. Fig. 9 shows results obtained with 75 %

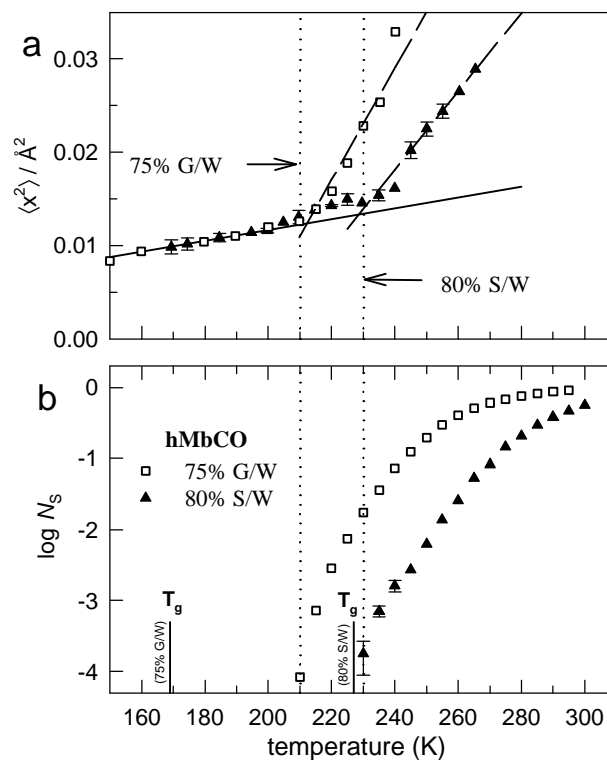


Figure 9:

- Mössbauer spectroscopy of ^{57}Fe substituted horse-myoglobin, iron mean square displacements in two solvents as indicated and
- the ligand escape fraction N_s , in the same solvents, kinetics of CO-binding to horse myoglobin, dashed lines are drawn to indicate the common onset temperatures. The short vertical lines denote the respective glass transition temperatures.

glycerol/water and 80 % sucrose/water: The latter is much more viscous than the former. Fig.(9a) displays the mean square displacements of the heme iron derived from the elastic intensity of the Mössbauer spectrum using the Gaussian approximation of equ.(1). We observe a dynamical transition which depends however on the properties of the solvent. The transition temperatures, 180 K (figs.2,3, water), 210 K (75% glycerol-water) and 230 K (80% sucrose-water) increase with increasing viscosity of the solvent.

This result suggests that the dominant contribution to the displacements of the heme iron depends on the external solvent viscosity.

The heme interacts with the solvent through its propionic acid side-chains. MD simulations indicate that lateral displacements of the heme as a whole in the protein cleft are much larger than the iron displacements relative to the heme plane [38]. The viscosity in associating liquids depends, apart from steric factors, on the hydrogen bond strength. This implies that both, the α - and the β -process will be delayed by an increase in the viscosity. The transition in fig.(9a) thus involves both components, consistent with a more detailed analysis of the spectra [37]. In the sucrose sample however we notice a pretransition at about 200 K. This interesting result may indicate that by strengthening the external H-bonds, we may separate the mobility transitions of internal and external hydrogen bonds.

Fig.(9b) shows the correlation of the heme displacements to those of the ligand CO (carbon monoxide). The kinetics of ligand binding has been studied using flash photolysis [23]. A simplified scheme which describes the kinetics at high temperatures involves only three ligand states: the bound state, Mb-CO, an geminate pair state, Mb(CO), with the ligand residing in the heme pocket and Mb+CO, the dissociated pair state:



The so-called escape fraction N_S describes how many ligand escape after photolysis from the heme pocket Mb(CO) to the solvent, Mb + CO, instead of rebinding directly. We have shown that the escape rate k_{out} depends on the external solvent viscosity, while the rate of geminate recombination, k_{gem} of Mb(CO) \rightarrow Mb-CO, is solvent independent [23]. The escape fraction thus decreases with increasing solvent viscosity η , or decreasing temperature: $N_S(\eta) = k_{out}(\eta) / (k_{out}(\eta) + k_{gem})$. This explains the data in fig.(9b). The identical shifts observed in the onset temperatures of the two solvents demonstrates that both, the heme and the ligand in the heme pocket interact with density fluctuations at the protein surface. In contrast, the direct association of CO with the heme iron, which involves a displacement of the iron with respect to the heme plane, is found to be independent of the solvent viscosity. It was proposed however, that intramolecular H-bond fluctuations trigger the final binding step by modulating the heme geometry [40].

7. Summary

The nonlinear increase in the mean square displacements was first observed for the heme iron with myoglobin crystals [12]. Bachleitner et al. [10] interpreted this effect as a glass transition triggered by the protein hydration shell. The more general notion of a dynamical transition was introduced 10 years to characterize the cross-over between two regimes dominated either by vibrational or diffusive structural displacements [11]. It is now established as a generic feature of protein dynamics [13,17,18,20,41], implying that a continuous change in the environmental and structural parameters beyond a critical value induces a discontinuous behaviour in the dynamical properties. This definition excludes structural phase transitions as the physical origin of the dynamic discontinuity. Further, the temperature where the anharmonic displacements start to emerge does not depend on the inherent time scale of the experimental setup. The associated fluctuation spectra resemble those observed with undercooled liquids [9]. Finally, the dynamical transition in proteins occurs even without solvent suggesting an intrinsic mechanism. The main intention of this article was to stress the role of polar interactions and water in particular using simple molecular models of protein structural fluctuations.

References

- [1] T. Takano, *J.Mol.Biol.* **110**:569-584 (1977)
- [2] D. Case and M. Karplus, *J.Mol.Biol.* **132**:343-368 (1979).
- [3] R. H. Austin et al. *Biochem.* **14**: 5355-5373 (1975)
- [4] H.Frauenfelder and P.Wolynes, *Science* **226**:337-345 (1985)
- [5] J.Wong and C.A.Angell, *Glass Structure by Spectroscopy*, Marcel Dekker, New York (1976)
- [6] W. Götze and L. Sjögren, *Rep.Prog.Phys.* **55**:241-376 (1992)
- [7] W. Götze, *J. of Phys.: Condensed Matter*, in press (1999)
- [8] W. Doster et al. in *Dynamics of Disordered Solids*, Springer Proceedings of Physics **37**:120-123 (1988)
- [9] W.Doster et al. *Phys.Rev.Lett.* **65**:1080-1084 (1990)
- [10] T. Bachleitner et al. *Biophys.J.* **50**:213-219 (1986)
- [11] W.Doster, S. Cusack and W. Petry, *Nature* **337**:754-758 (1989)
- [12] F. Parak and H. Formanek, *Acta Cryst.* **27A**:573-578 (1971)
- [13] J.L. Green, J. Fan and C.A. Angell, *J.Phys.Chem.* **98**:1378-13790 (1994)
- [14] Sartor et al. *J.Phys.Chem.* **96**:5133 (1992)
- [15] Doster et al. in *Water-Biomolecules Interactions*, *Ital.Phys.Soc. Proceedings* **43**:123-126 (1993)
- [16] J. Smith, K. Kuczera and M. Karplus *PNAS, USA* **87**:1601-1605 (1990)
- [17] U. Lehnert et al. *Biophys.J.* **75**:1945-1952 (1998)
- [18] J. Fitter, R.E. Lechner and N.A. Dencher *Biophys.J.***73**:2126-2137 (1997)
- [19] F. Sciortino et al. *Phys.Rev.Lett.* **64**:1686-1689 (1990)
- [20] F. Demmel et al. *Europ.Biophys.J.* **26/4**:327-336 (1997)
- [21] E.N. Baker and R.E. Hubbard, *Prog.Biophys.Molec.Biol.* **44**:98-180 (1984)
- [22] X. Cheng and B. Schoenborn, *Acta Cryst.* **B46**:195 (1990)
- [23] T. Kleinert et al., *Biochem.* **37**:717-733 (1998)
- [24] Diehl et al., *Biophys.J.***73**:2726-2732 (1997)
- [25] M. Bee, *Quasielastic Neutron Scattering*, Adam Hilger (1988)
- [26] R.F. Tilton, J.C. Dewan and G.A. Petsko, *Biochem.* **31**:2469-22481 (1992)
- [27] F. Parak et al. *Eur.Biophys.J.* **16**:237-249 (1987)
- [28] T.D. Romo et al. *Proteins*, **22**:311-321 (1995)
- [29] G. Kneller et al. *J.Chem.Phys.*, **97**:8864-8879 (1992)
- [30] E.R. Bauminger et al. *Proc.Natl.Acad.Sci. USA*, **80**:736-740 (1983)
- [31] M. Settles and W. Doster in *Biological Macromolecular Dynamics* p. 3-8, .Adenine Press,1996
- [32] M. Settles, Thesis, Technische Universität München (1996)
- [33] F. Parak, J. Heidemeier and U. Nienhaus, *Hyperfine Interactions* **40**:147-158 (1988)
- [34] J.A. Jeffrey and W. Saenger in *Hydrogen Bonding in Biological Structures*, Springer Verlag (1991)
- [35] H. E. Stanley and J. Teixeira, *J.Chem.Phys.* **73**:3404-3422 (1980)
- [36] D. Bertolini et al. *J.Chem.Phys.* **91**:1179 (1989)
- [37] H. Lichtenegger et al. *Biophys.J.***76**:99030 (1999)
- [38] K. Kuczera, J.Kuriyan and M. Karplus, *J.Mol.Biol.* **213**:351-373 (1990)
- [39] X. Huang and S.G. Boxer, *Nature Struct.Biol.* **1**:226-229
- [40] W. Doster, *Europ.Biophys.J.* **17**:217-220 (1989)
- [41] C. Andreani et al. *Biophys.J.* **68**:259 (1995)
- [42] I. Iben et al. *Phys.Rev.Lett.*, **62**:1916-1919 (1989)
- [43] M.-C. Bellissent-Funel et al. *J.Phys. I France* **2**:995-1001 (1992)
- [44] E.W. Knapp, S.F. Fischer and F. Parak *J.Phys.Chem.* **86**:5042-5047 (1982)